The wurtzite to rock salt structural transformation in CdSe nanocrystals under high pressure

Sarah H. Tolbert and A. P. Alivisatos
Materials Sciences Division, Lawrence Berkeley Laboratory and Department of Chemistry, University of California, Berkeley, California 94720

(Received 22 September 1994; accepted 8 December 1994)

Structural transformations in CdSe nanocrystals are studied using high pressure x-ray diffraction and high pressure optical absorption at room temperature. The nanocrystals undergo a wurtzite to rock salt transition analogous to that observed in bulk CdSe. Both the thermodynamics and the kinetics of the transformation, however, are significantly different in finite size. The nanocrystal phase transition pressures vary from 3.6 to 4.9 GPa for crystallites ranging from 21 to 10 Å in radius, respectively, in comparison to a value of 2.0 GPa for bulk CdSe. The size dependent data can be modeled using thermodynamics when surface energies are accounted for. Surface energies calculated in this way can be used to understand the dynamic microscopic path followed by atoms during the phase transition. X-ray diffraction data also shows that unlike bulk CdSe, crystalline domain size is conserved upon multiple transition in the nanocrystals, indicating that the transition only nucleates once in each nanocrystal.

I. INTRODUCTION

Recent studies of clusters in both the gas and condensed phases show multiple examples of novel bonding geometries, many of which differ from those observed in bulk systems.[1] The existence of these unique structures opens up the general question of the effects of physical size on structural stability in nanometer size solids. As the total extent of a material is decreased from the bulk limit to systems containing only a few hundred atoms, how will the relative stability of different possible solid structures change?

One way to answer this question is to use pressure to force finite size materials to convert from one solid structure to another, a technique frequently used in bulk solids to assess the relative stability of various crystal structures. In extending these experiments to finite systems, a number of factors are potentially important. Three questions in particular will be addressed in this paper: (1) To what extent can pressure induced solid–solid structural transformations be used to understand the relative stability of various solid structures in finite size? (2) How will the transition kinetics differ in finite size, as compared to bulk solids? (3) What can be learned about the basic nature of solid–solid phase transitions by studying finite systems?

The surface energy of a nanocrystal can play a dominant role in determining the stable phases. In melting studies on a wide variety of nanocrystal materials, a depression in melting temperature is observed with decreasing size. The data can be quantitatively explained by the notion that the liquid phase is stabilized relative to the solid because the cluster surface energy is lower in the liquid phase.[2,3] In an attempt to answer question (1) above, we will apply these surface tension ideas to solid–solid phase transitions. The results, combined with a general understanding of surface structure and surface energy, will be used to address questions (2) and (3).

The system that we have chosen for these experiments is CdSe semiconductor nanocrystals. In this paper we extend our previous work[4] on high pressure transformations in CdSe nanocrystals. These crystallites can be synthesized with very narrow size distributions and high crystallinity in sizes ranging from 10 to 30 Å in radius.[5,6] The high quality of these samples makes them ideal for studying the effect of size on structural stability.

Bulk CdSe is known to undergo a wurtzite to rock salt transition at 2.0 GPa.[7] The transition is accompanied by a 20% decrease in unit cell volume and a change in coordination number from 4 to 6. In CdSe (Refs. 8 and 9) and CdS (Refs. 10 and 11) nanocrystals, however, it has been observed that the low pressure wurtzite structure is stable to pressures much higher than the bulk transition pressure. In GaAs/AlAs superlattices[12] an elevation of the AlAs phase transition pressure has also been observed. Neither the CdS/Se nanocrystal nor the superlattice experiments, based on either Raman or optical absorption, determined the high pressure phase structure, or the degree of crystallinity in the high pressure phase. Also, due to limits in the ability to chemically synthesize II–VI nanocrystals, earlier experiments investigated only one size nanocrystal, and samples contained a broad size distribution. Advances in synthetic methods have now removed these constraints.[5,6]

Recently, we have applied high pressure Se EXAFS to the question of understanding the transformed structure in these crystallites.[13] Unlike x-ray diffraction where large Debye–Scherrer broadening makes experiments on small samples very difficult, EXAFS probes short range order and so quality EXAFS data can be collected on very small nanocrystal samples. These experiments were limited, however, in that they could not assess the degree of crystallinity in transformed samples, and they could only suggest that, by analogy with bulk CdSe, a rock salt structure was reasonable for the high pressure phase.

In this paper we have thus chosen to apply a combination of high pressure x-ray diffraction and high pressure optical absorption to the study of solid–solid structural transformations in CdSe semiconductor nanocrystals. These techniques allow us to determine both the structure and de-

 0021-9606/95/102(11)/4642/15/$6.00

gree of crystallinity of the nanocrystals in every phase, as well as the dependence of the transformation pressure on nanocrystal size. The experiments show that the phase transition pressure is elevated in finite size, but that the nanocrystal domain size is conserved upon transition. These results have important implications for theories of solid–solid phase transitions in both nanocrystalline and bulk systems. More importantly, this combination of experiments allows us to separate thermodynamic from kinetic effects and thus gain some real understanding of the factors that control stability in finite size.

II. EXPERIMENT

Bulk CdSe samples, which had been annealed to reduce structural faults, were obtained from Cleveland Crystals. The CdSe nanocrystals used in this experiment were prepared chemically using a modification of the method of Murray and Bawendi.[5,6] Crystallites were characterized using x-ray powder diffraction, transmission electron microscopy (TEM), x-ray photoelectron spectroscopy (XPS), optical absorption, and Raman scattering. TEM shows that these nanocrystals are nearly spherical, although facets can be observed in crystallites over 30 Å in diameter.[14] Detailed surface characterization was performed using XPS (Ref. 6) and NMR;[15] CdSe nanocrystals dissolved in pyridine appear to have surface Cd atoms which are coordinated to solvent nitrogen atoms. Some small fraction of the surface Se atoms are bonded as tri-alkyl-phosphine-selenide. In addition, some small fraction of the surface Cd and Se atoms could be present as oxides. The total number of bound ligands appears to be limited by steric effects between ligands and not by the availability of unbound surface sites.

Crystallite size and size distributions were determined using TEM, x-ray diffraction, and small angle x-ray scattering (SAXS). The samples used in this experiment were found to be wurtzite in structure with an average size dispersion of σ=5%. Only samples which were shown to be free of stacking faults by comparison of x-ray diffraction Debye–Scherrer peak widths and TEM/SAXS sizes were used in these experiments. A sample diffraction pattern for 2.2 nm radius CdSe nanocrystals is shown in Fig. 1. The symbols indicate the experimental data. The solid line is a calculated pattern based on the size determined by TEM/SAXS and the assumption of spherical nanocrystals. Residuals are included to emphasize the agreement.

High pressure optical absorption data was obtained using a scanning Cary model 118 UV/visible spectrometer in combination with a Mao-Bell-type diamond anvil cell (DAC) with spring steel gaskets and 0.2 mm diam sample chambers. Nanocrystals were dissolved in 4-ethyl-pyridine, a solvent which has been shown to be a reasonable quasihydrostatic pressure medium to pressures in excess of 10 GPa, and in which the nanocrystals are extremely soluble. Pressure was determined using ruby fluorescence. In all cases, multiple fluorescence measurements were taken at various locations in the cell and pressure gradients were shown not to exceed 10%.

High pressure x-ray diffraction experiments were carried out on wiggler beam line 10-2 at the Stanford Synchrotron Radiation Laboratory (SSRL). Focused monochromatic 12.5 keV x-rays were collimated and apertured to a 0.1 mm beam through a series of 3 slits and pinholes. The x-ray energy was chosen to be below the Se absorption edge (12.6 keV), thus minimizing Se absorption and K-α fluorescence. A Merrill-Bassett style diamond cell with Be rockers was used in combination with inconel gaskets. The cell was positioned at the center of a Huber 6 circle diffractometer which provided precise positioning of the cell with respect to the x-ray beam. Diffracted x-rays were collected on Fuji image plates and read with 0.1 mm resolution. Typical integration times ranged from 30 min to 1 h, with diffraction intensities being a strong function of sample alignment. Debye–Scherrer rings were angle integrated to produce the data presented here. Like the optical absorption experiments, nanocrystal samples were dissolved in 4-ethyl-pyridine and standard ruby fluorescence techniques were used to determine pressure.

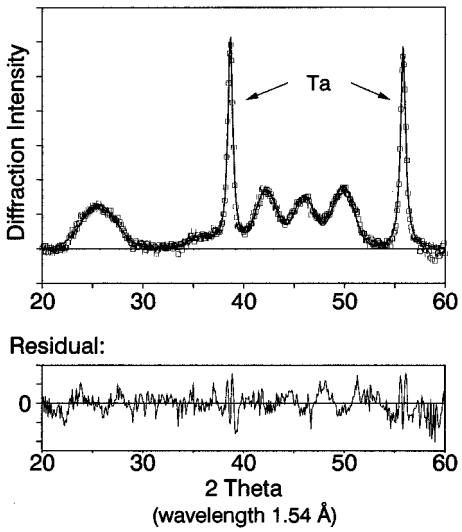

FIG. 1. Atmospheric pressure x-ray diffraction pattern from 4.2 nm diam CdSe nanocrystals. Open squares represent data. The solid line is calculated based on the assumption of spherical nanocrystals and the nanocrystal size determined by TEM/SAXS. Residuals are included to emphases the agreement. Tantalum diffraction peaks are from the sample holder.

III. RESULTS

A. High pressure x-ray diffraction

High pressure x-ray diffraction data collected on bulk CdSe is presented in Fig. 2(a). The system is observed to be completely transformed from a low pressure wurtzite[16] structure to a high pressure rock salt[17] structure by 3.5 GPa. This is in good agreement with values of 3.0 GPa upstroke for the bulk CdSe wurtzite to rock salt phase transition pressure presented in the literature.[7,18] Upon release of pressure, a tetrahedral structure is recovered, though it appears to be a mix of zinc blende[19] and wurtzite. This is also in agreement with previous observations.[7(b),7(c)] Intensity anomalies in the untransformed wurtzite peaks [Fig. 2(a)] are due to single crystal diffraction effects from the finite number of grains in the sample. The crystalline domain size decreases as the system undergoes subsequent transition [Fig. 2(a)], starting with an

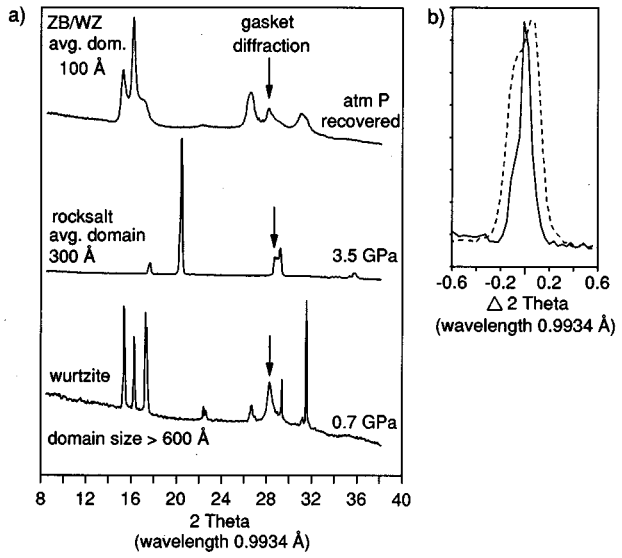

FIG. 2. (a) High pressure x-ray diffraction data obtained on bulk CdSe. The sample is initially in the wurtzite phase. By 3.5 GPa, the sample has transformed to the rock salt phase. Upon release of pressure, a wurtzite/zinc blende mixed phase is recovered. Intensity anomalies in the original wurtzite pattern are due to single crystal effects caused by the finite number of grains in the sample. The arrow indicates diffraction from the metal gasket of the diamond cell. Domain size labels indicate the average domain size in each phase, and show a decrease in domain size with each transition. (b) Blowup of the original wurtzite (002) peak (solid line), and the rock salt (111) peak (dashed line). See Fig. 4 for indexing. The data are plotted as $\Delta 2\theta$ with respect to the wurtzite and rock salt peak centers of 16.42 and 17.76 2θ, respectively. The marked broadening of the rock salt peak compared to the wurtzite is cause by a decrease in domain size upon phase transition.

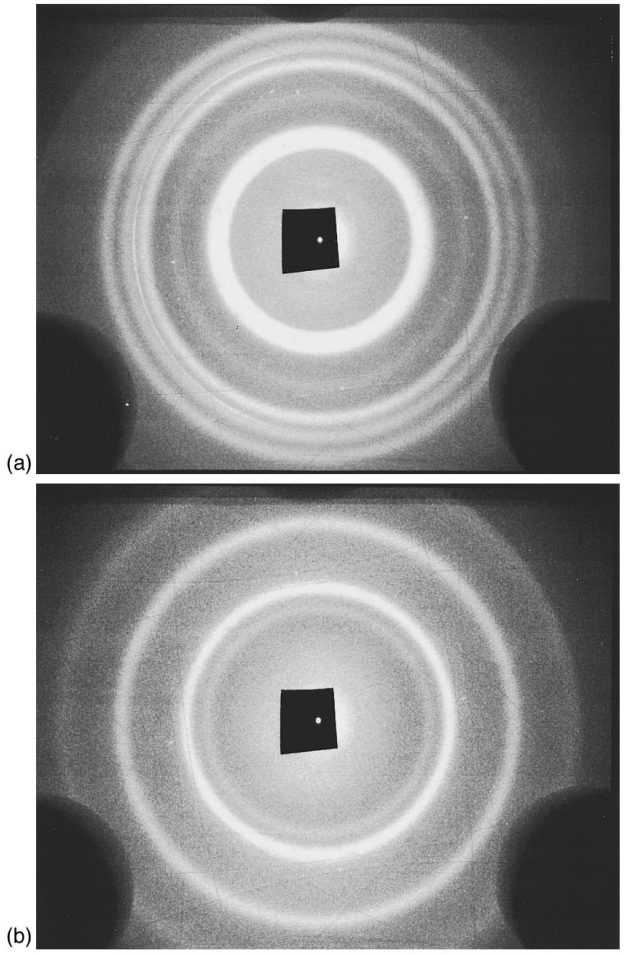

FIG. 3. Raw diffraction data obtained on 4.2 nm diam CdSe nanocrystals in the (a) wurtzite (1 GPa) and (b) rock salt (10 GPa) phases. Debye–Scherrer rings of this type are angle integrated to produce the data presented in Figs. 2, 4–6, and 8.

instrument limited domain size greater than 600 Å (actual size=~1 μm); decreasing to about 300 Å in the rock salt phase, and then further decreasing to approximately 100 Å in the recovered tetrahedral phase. Diffraction peaks from the original wurtzite phase and the transformed rock salt phase have been expanded in Fig. 2(b) to emphasize this change in peak width. The broadening in the recovered zinc blende/wurtzite phase is clearly seen in Fig. 2(a). This observation will be discussed further in the next section.

Raw diffraction data obtained on 21 Å radius CdSe nanocrystals in the wurtzite and rock salt phases are shown in Fig. 3. Debye–Scherrer rings were angle integrated to produce the patterns presented in Figs. 2, 4–6, and 8. The angle integration increases the relatively poor signal to noise observed in the raw data by over an order of magnitude. Averaged data obtained on the same 21 Å radius nanocrystals is presented in Fig. 4. In contrast to bulk CdSe, the sample is observed to retain the wurtzite structure well above the bulk phase transition pressure of 3 GPa upstroke. At pressures above 6 GPa, the sample begins to convert to the rock salt structure. The coexistence of both phases is observed in the 6.3 GPa scan. The two phase stability is in part due to small pressure gradients in the DAC. Additionally, some inhomogeneity in sample size and surface structure could contribute to the observed two phase coexistence. Upon further application of pressure a clean rock salt pattern is observed. There is excellent agreement in terms of rock salt peak positions and relative intensities between the nanocrystal and bulk CdSe spectra. Upon release of pressure (Fig. 5), the transition is found to be highly hysteretic. The rock salt structure remains stable to pressures significantly below the observed upstroke transition pressure. By 1 GPa, however, the sample does begin to recover, and by atmospheric pressure, a mixed zinc blende/wurtzite pattern is recovered, again in good agreement with bulk CdSe.

Significantly different from the bulk, however, is the observation presented in Fig. 6 that the diffraction peak widths do not significantly increase upon transition from the wurtzite structure to the rock salt and back to wurtzite/zinc blende. The domain size is unchanged upon transition from wurtzite (average size=41 Å) to rock salt (average size=42 Å), and only slightly decreases on the reverse transition (average size=38 Å). These data suggest that nanocrystals are coherently transforming from one solid structure to another. The significance of this observation will be addressed in the discussion.

The data presented in Figs. 4 and 5 can be fit to obtain peak positions as a function of pressure (Fig. 7). These data can then be used to determine the bulk modulus (B_0) in the rock salt phase. B_0 is defined as the reciprocal of the volume compressibility. The experimentally determined value for the

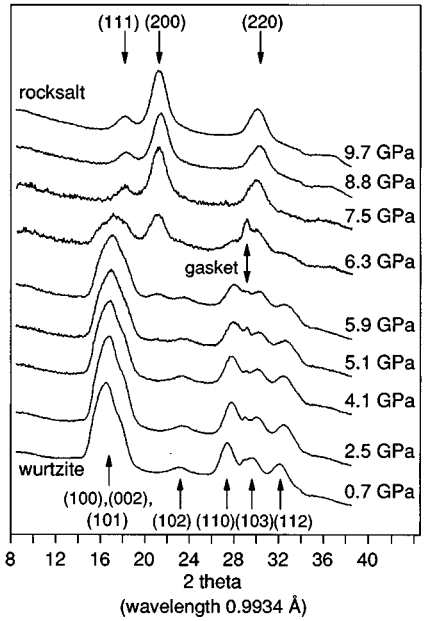

FIG. 4. High pressure x-ray diffraction data obtained on 4.2 nm diam CdSe nanocrystals with increasing pressure. Pressures and indexing for both the wurtzite and rock salt phases are indicated on the figure. The nanocrystals are observed to transform to the rock salt phase at approximately 6 GPa, which is twice the bulk upstroke transition pressure. The arrow indicates diffraction from the metal gasket of the diamond cell.

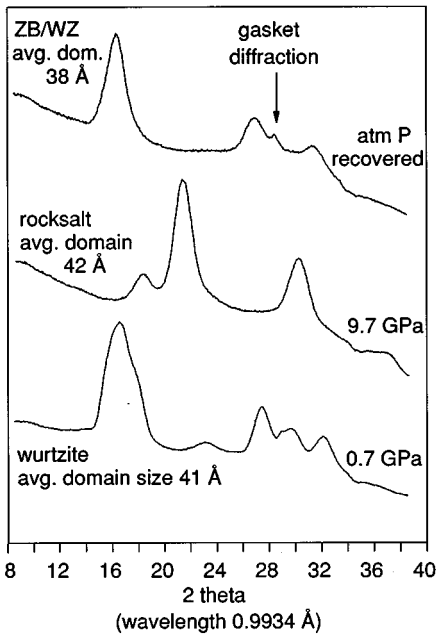

FIG. 6. High pressure x-ray diffraction data obtained on 4.2 nm diam CdSe nanocrystals in the untransformed wurtzite phase, the high pressure rock salt phase, and the recovered zinc blende/wurtzite mixed phase. In contrast to bulk CdSe (Fig. 2), domain size labels show that there is essentially no change in domain size after multiple transitions.

rock salt phase nanocrystals of $B_0=74\pm2$ GPa is in reasonable agreement with other reported values for bulk and nanocrystalline CdSe.[13,20] Unfortunately, due to the overlap of the many wurtzite diffraction peaks, it was not possible to obtain an accurate value of B_0 for the wurtzite phase. The wurtzite data are, however, consistent with our previous values obtained from high pressure Se EXAFS experiments on CdSe nanocrystals.[13]

To insure that conclusions based on data obtained on 21 Å radius nanocrystals were generalizable to smaller sized crystallites, a limited data set was collected on 10 Å radius nanocrystals as well (Fig. 8). In good agreement with the results for larger crystallites, these nanocrystals were observed to transform from a wurtzite phase to a rock salt

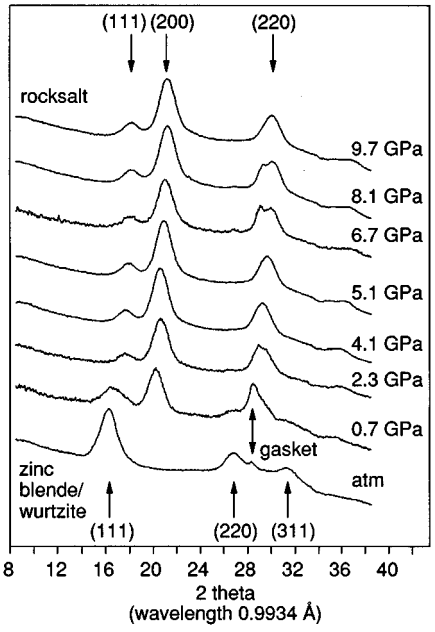

FIG. 5. High pressure x-ray diffraction data obtained on 4.2 nm diam CdSe nanocrystals with decreasing pressure. Pressures and indexing for both the rock salt and zinc blende phases are indicated on the figure. The nanocrystals are observed to transform from the rock salt phase to a mixed zinc blende/wurtzite phase at approximately 1 GPa. The arrow indicates diffraction from the metal gasket of the diamond cell.

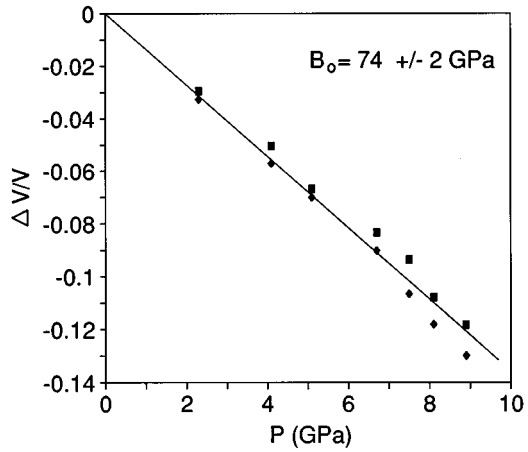

FIG. 7. Fractional shift in unit cell volume with pressure for the rock salt phase of 4.2 nm diameter CdSe nanocrystals. Square and diamond markers correspond to data obtained using the (220) and (200) diffraction peaks, respectively. The data can be fit with a linear volume compressibility of $B_0=74\pm2$ GPa.

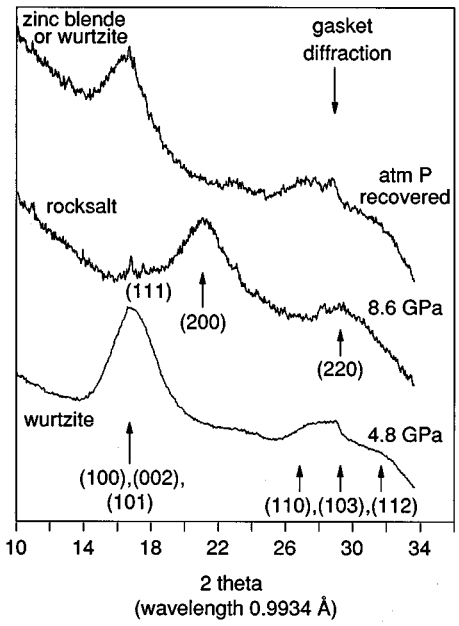

FIG. 8. High pressure x-ray diffraction data obtained on 1.9 nm diam CdSe nanocrystals in the untransformed wurtzite phase, the high pressure rock salt phase, and the recovered tetrahedral phase. Pressures and indexing for both the wurtzite and rock salt phases are indicated on the figure. The arrow indicates diffraction from the metal gasket of the diamond cell. The data shows no increase in domain size upon multiple transitions, and indicates that results obtained on 4.2 nm diam nanocrystals are generalizable to smaller crystallites.

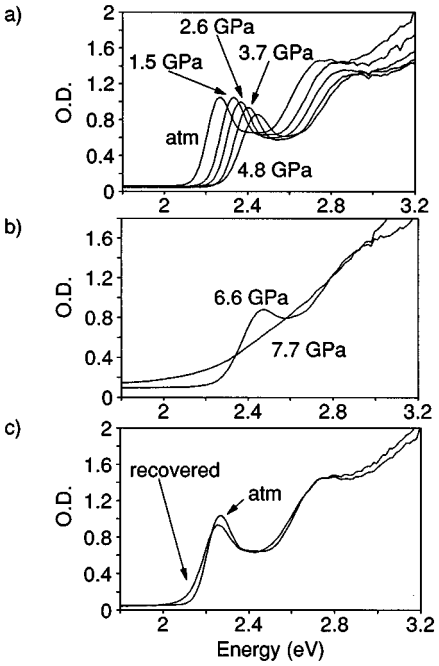

FIG. 9. High pressure optical absorption obtained on 2.8 nm diam CdSe nanocrystals at high pressure. (a) shows the shift in the wurtzite phase absorption with pressure. (b) demonstrates that optical absorption can be used to determine the phase transition pressure. The direct gap wurtzite feature disappears and is replaced by a featureless absorption which can be assigned to the indirect gap of the rock salt phase. (c) shows that upon release of pressure, the direct gap features are recovered. All spectra have been normalized for changes in o.d. due to deformation in the diamond cell gasket.

phase by 8.6 GPa, and back to a tetrahedral structure. Due to the extreme Debye–Scherrer broadening in these clusters, it is not possible to distinguish between possible tetrahedral structures in the recovered sample. Within the limits of the data, however, there does not appear to be any significant broadening of the diffraction peaks upon multiple transitions.

B. High pressure optical absorption

While the effect of pressure on optical absorption in these systems is an interesting question, it is not the focus of this paper, and thus will not be discussed in detail.[21] Optical absorption is used here simply to identify the extent of transformation with varying pressure. High pressure optical absorption data obtained on 14 Å radius CdSe clusters are presented in Fig. 9. The data presented here have been corrected for intensity changes due to deformation of the DAC gasket. These corrections are determined by observing the changes in diameter and thickness of the gasket hole for a typical gasket using an optical microscope and the thin film interference between the diamond surfaces. Volume and thickness changes were related to variations in concentration and path length, and these effects were corrected for using Beer's law. Fig. 9(a) shows the shift in the first confined wurtzite phase exciton transition with increasing pressure. The magnitude of this shift is observed to be fairly constant over a wide range of nanocrystal sizes.

Figure 9(b) shows the disappearance of the confined absorption peak at the phase transition pressure. The featureless absorption spectra in the high pressure phase is consistent with a high pressure rock salt structure, which is predicted to be an indirect, narrow gap semiconductor. The optically determined phase transition pressure is observed to correlate extremely well with the structural phase transition pressure determined by high pressure x-ray powder diffraction. This correlation allows for the routine assessment of phase transition pressures on multiple sizes of nanocrystals using simple optical techniques in our own laboratory. In Fig. 9(c), the confined direct gap absorption is shown to return upon release of pressure. This result is in good agreement with the complete recovery of the tetrahedral phase observed in x-ray diffraction and the observation that the domain size, and thus the confinement size, is not altered. No significant loss of oscillator strength is observed in the optical spectra upon reverse transition, though some broadening of the peak has occurred. The increased tail to the red in the recovered peak could be due to an elevated number of surface states, formed through the rearrangement of the surface with multiple transitions at room temperature.

The hysteresis observed in Figs. 4 and 5 can be quantified using optical absorption. Hysteresis curves for 3 sizes of CdSe nanocrystals are presented in Fig. 10. These data are obtained by integrating the lowest energy direct gap optical transition in both upstroke and recovered samples. As in Fig. 9, these data have also been corrected for changes in o.d. due to deformation of the DAC cell gasket. The ''fraction rock salt'' value is calculated from the integrated direct gap peak area assuming 100% wurtzite at low pressures and 100%

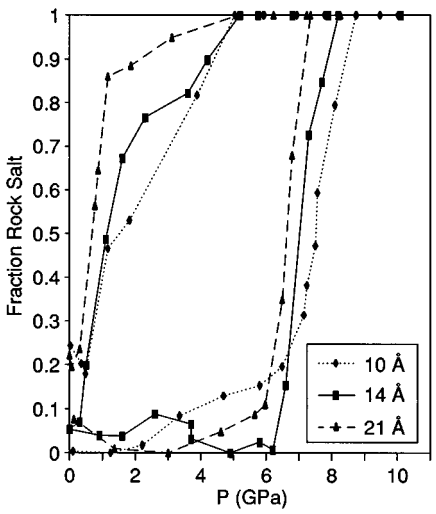

FIG. 10. Hysteresis curves for three sizes of CdSe nanocrystals. Data were obtained by integration of the low pressure phase absorption features shown in Fig. 9. "Fraction rock salt" is defined as 1-(fractional wurtzite phase absorption). Phase transition pressures are assigned to the midpoints of these hysteresis curves.

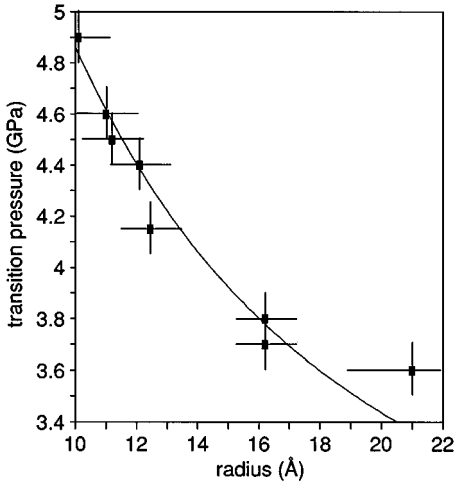

FIG. 11. Wurtzite to rock salt transformation pressure as a function of CdSe nanocrystal radius. The transition pressures are defined according to Fig. 10. The solid line is a fit to the thermodynamic model explained in Secs. IV A 1, IV A 2, and the Appendix.

rock salt at very high pressure. The apparent incomplete recovery of some of the samples is probably due to variations in the way gaskets deform with each experimental run. The up and down stroke phase transition pressures are assigned to the 50% transformed point for both increasing and decreasing pressure. A smooth trend with size is observed with smaller clusters transforming to, and recovering from, the rock salt phase at higher pressures than larger clusters. The widths of all of these hysteresis curves are, however, significantly broader than those observed for bulk CdSe in high pressure resistivity measurements. Bulk CdSe shows an upstroke transition near 3 GPa, and a reverse transition at 1 GPa.[7] Some size dependence is observed in the sharpness of the hysteresis curves, particularly for the downstroke transitions; smaller sizes appear to recover more gradually.

The nanocrystal size dependence of the wurtzite to rock salt phase transition pressure can be obtained by assigning the phase transition pressure to the midpoint of the hysteresis curve. The data are presented in Fig. 11. The monotonic increase in phase transition pressure with decreasing nanocrystal size suggests a systematic mechanism for this high pressure behavior. The exploration of possible mechanisms for this increase will be the focus of the remainder of this paper.

IV. DISCUSSION

Can pressure induced solid–solid phase transitions be used to understand the relative stability of various solid structures in finite size? We attempt to answer this question in the first section of the discussion (Thermodynamics), where the ideas of surface thermodynamics are used to calculate surface energies in wurtzite and rock salt phase nanocrystals. In the next section (Kinetics), these surface energies are used to postulate the dynamic path followed by atoms during the phase transition. Here we attempt to answer two questions. How do transition kinetics differ in finite size, as compared to the bulk? And what can we learn about the effect of kinetics on solid–solid phase transitions by studying finite systems?

A. Thermodynamics

1. Thermodynamic arguments

Much understanding of the elevated phase transition pressures observed in these systems can be gained by using thermodynamics to model the transformation.[10,13] The observation that nanocrystal compressibilities, in both the wurtzite and rock salt phases, are almost identical to bulk compressibilities, argues that there is no intrinsic size effect in the stability of the nanocrystal interior. It is thus permissible to use bulklike thermodynamic arguments to describe the observed solid–solid phase transitions in these nanocrystals. Bulk thermodynamic expressions, however, need to be modified by surface energy terms to describe our nanophase materials.

In this nanocrystalline system, as in bulk CdSe, we will assume that the wurtzite and zinc blende structures are approximately isoenergetic, and so the recovered wurtzite/zinc blende mixed phase will be treated as thermodynamically equivalent to the original pure wurtzite structure. This assumption is justified by the fact that in CdSe and CdS, zinc blende to rock salt and wurtzite to rock salt phase transitions are observed to occur at close to the same pressures.[7(b),22] The thermodynamic arguments, presented in some detail for a single size of nanocrystal in previous publications,[10,13] are summarized in the Appendix and generalized to predict the nanocrystal size dependence of the phase transition pressure.

The internal energies for the high and low pressure phases of the nanocrystals are given by

$$U_{\mathrm{WZ}}(P,V) = TS_{\mathrm{WZ}} - PV_{\mathrm{WZ}} + \mu_{\mathrm{WZ}}N_{\mathrm{WZ}} - \gamma_{\mathrm{WZ}}A_{\mathrm{WZ}}$$
$$U_{\mathrm{RS}}(P,V) = TS_{\mathrm{RS}} - PV_{\mathrm{RS}} + \mu_{\mathrm{RS}}N_{\mathrm{RS}} - \gamma_{\mathrm{RS}}A_{\mathrm{RS}}, \quad (1)$$

TABLE I. Physical constants used in thermodynamic calculations. Here B_0 is the bulk modulus, B_0' is the derivative with the bulk modulus with respect to pressure, and V_0 is the primitive unit cell volume at atmospheric pressure. The c_1 and c_2 terms are used to calculate the surface energy in a nanocrystal, as defined in Eq. (2). They are the flat surface and curvature terms, respectively. All of the constants are determined independently, except for $c_{1,RS}$ and $c_{2,RS}$, which are obtained by a fit to the size dependent phase transition data.

Physical constants	Wurtzite	Rock salt
B_0 (GPa)	37±5	74±2
B_0'	11±3	
V_0 (m^3)	5.62×10^{-29}	4.36×10^{-29}
c_1 (N/m)	0.34	0.63
c_2 (N/m) ($Å^2$)	84	83

where U, S, and μ are the bulklike internal energy, entropy, and chemical potential terms, respectively, for each phase, and γ and A are the nanocrystal surface tensions and surface areas for each phase.

The exact form of γ is an important, although not well established issue. However, recent observations of faceted nanocrystals suggest that it may be possible in the future to exactly determine γ_{WZ}.[14] For these experiments, the surface energy in each phase is assumed to vary as

$$\gamma_i = c_{1,i} + \frac{c_{2,i}}{r(Å)^2}. \tag{2}$$

Here the c_1 term corresponds to the bulk surface energy of some hypothetical average low index surface. In the limit of large size, only the c_1 term remains. The c_2 term corresponds to the increase in surface energy due to the curvature of the cluster. For spherical systems (which are a reasonable approximation of our nanocrystals), this term varies at $1/r^2$. The c_2 term can be thought of as the increase in γ caused by steps and edges which must be induced in a low index surface in order to make it curve into a sphere. An analogous formalism with a similar radius dependence is used to describe the effect of curvature on the surface energy of micelles.[23]

Assuming wurtzite/rock salt equilibrium, the expressions for U_{WZ} and U_{RS} in Eq. (1) can be combined. Thermodynamic relations can then be used to re-express Eq. (1) in terms of phase transition pressures, compressibilities, and surface energies, most of which are experimentally determinable (Table I). The details of this process are presented in the Appendix. The goal is to compare phase transition data, collected on a variety of nanocrystal sizes, with this thermodynamic model. This process can be used to understand the nanocrystal size dependence of the phase transition pressure, and to calculate nanocrystal surface energies in the rock salt phase.

This thermodynamic model can, however, be explained on a more intuitive level by considering the energy–volume plane[24,10] (Fig. 12). In the formalism of the Appendix, an energy–volume curve can be drawn for each phase of CdSe. Theoretically, one should plot the Helmholtz energy, A, vs volume. Because we have chosen to ignore entropy effects, however (see the Appendix), we are actually plotting the internal energy, U, vs volume. On this plane, pressures are represented by straight lines of a given slope ($-dU/dV = P$). The bulk rock salt curve is observed to be offset from the bulk wurtzite curve to higher energy and smaller volume. A line which corresponds to the bulk phase transition pressure of 2.0 GPa can be drawn tangent to these two curves. The wurtzite phase curve for any single size of nanocrystal is offset from the bulk wurtzite curve to higher energy because of the surface energy, and to slightly smaller volume because of a lattice contraction caused by this surface energy. Figure 12 shows these curves for bulk CdSe and 3 sizes of nanocrystals. The surface energy offset and the lattice contraction vary with crystallite size, with the smallest nanocrystals offset to the highest energy and smallest volume. The experimentally observed elevation in phase transition pressure with decreasing nanocrystal size can be simply understood by realizing that the surface energy in the rock salt phase must be higher than in the wurtzite phase. As the nanocrystal size decreases, the slope of the line needed to connect the rock salt and wurtzite curves increases, and thus the phase transition pressure increases. The fact that the nanocrystal curves in the wurtzite and rock salt phases are offset to both higher energy and smaller size, however, complicates the mathematical description of this relatively simple effect, and requires the more complex description presented in the appendix to actually compare theory and experimental data.

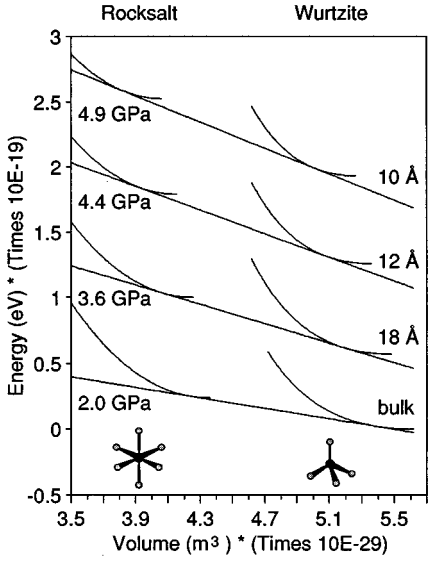

FIG. 12. Energy volume curves for bulk CdSe and three sizes of CdSe nanocrystals in both the wurtzite and the rock salt phases. Nanocrystal curves are offset with respect to the bulk due to the surface energy in the nanocrystals. The offset of the rock salt curves with respect to the wurtzite curves determines the phase transition pressure. Transition pressures and nanocrystal sizes are indicated on the figure.

2. Comparison to data

The equations presented in the Appendix can be combined to define an equilibrium equation that is a function of P_T, r_{WZ}, $c_{1,WZ}$, $c_{2,WZ}$, $c_{1,RS}$, and $c_{2,RS}$. Here P_T is the measured phase transition pressure, r_{WZ} is the wurtzite nanocrys-

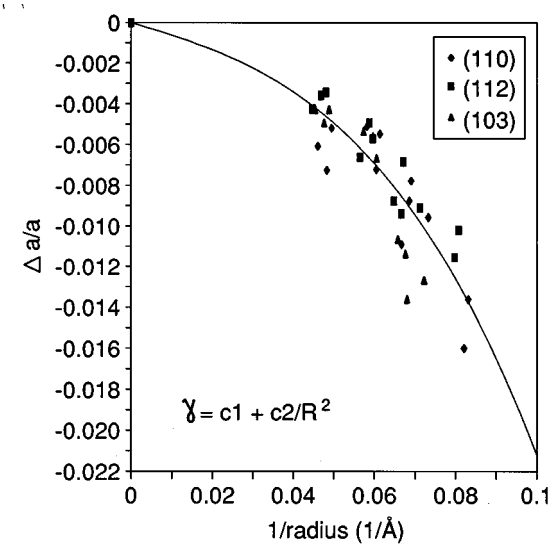

FIG. 13. Fractional change in CdSe lattice constant at atmospheric pressure, plotted against inverse nanocrystal radius. The data are fit with an $a_1/r+a_2/r^3$ dependence, which can be used in combination with the Laplace Law to calculate an average surface tension for the wurtzite phase nanocrystals (see text). The functional form for the surface tension is shown on the figure, and is numerically equal to $\gamma_{WZ}=0.34+84/r(\text{Å})^2$ (N/m), where the first term can be related to a bulk surface energy, and the second term is the elevation in γ due to the curvature of the nanocrystal. Square, diamond, and triangle markers represent data obtained using the (112), (110), and (103) diffraction peaks, respectively.

tal radius, and the c_1 and c_2 terms are the flat surface and curvature terms, respectively, used to define the nanocrystal surface energy in Eq. (2). The values of $c_{1,\mathrm{WZ}}$ and $c_{2,\mathrm{WZ}}$ can be determined experimentally from the size dependence of the lattice contraction at atmospheric pressure (Fig. 13) using the Laplace Law [Eq. (3)]. This equation relates the observed lattice contraction for a spherical cluster to the surface tension through the concept of a surface pressure,[25]

$$P_s=\frac{2\cdot\gamma(r)}{r}=\frac{\Delta a}{a}\cdot 3B_0. \tag{3}$$

Equation (3) is only rigorously correct for a completely homogeneous, spherical system with no surface structure, like a liquid droplet. The equation has been applied to nanocrystalline solids in the past, however, with some success.[26] With some hesitation, we will use this formalism to calculate a wurtzite phase surface energy. The data in Fig. 13 are fit with a $1/r+(1/r)^3$ dependence, obtained by substitution of Eq. 2 into Eq. (3). Good agreement is observed between the lattice contraction calculated from the wurtzite (112), (110), and (103) diffraction peaks. The resulting values are $c_{1,\mathrm{WZ}}=0.34$ and $c_{2,\mathrm{WZ}}=84$. The value of 0.34 N/m for the bulk surface energy term is close to the value for a zinc blende CdSe(111) single crystal surface of 0.55 N/m.[27] The difference could be a function of surface passivation by bound organic ligands and any reconstruction that may occur on the nanocrystal surface.

While the thermodynamic expressions presented in the Appendix still cannot be solved analytically for either $c_{1,\mathrm{RS}}$ or $c_{2,\mathrm{RS}}$ as a function of P_T and r_{WZ}, the equations can be compared to experimental data on $P_T(r_{\mathrm{WZ}})$ and the values of $c_{1,\mathrm{RS}}$ and $c_{2,\mathrm{RS}}$ varied to maximize the agreement between the experiment and the model. Experimental values for the phase transition pressure in both bulk CdSe and CdSe nanocrystals are obtained by averaging the upstroke and downstroke transition pressures. Assigning the thermodynamic transition pressure in this way assumes symmetric contributions (over- vs underpressing) to the thermodynamic driving force for transition $[\Delta V_{\mathrm{trans}}\cdot(P_{\mathrm{trans,thermo}}-P_{\mathrm{trans,exp}})]$. For transitions which may involve mechanical instability, like this one, the assumption of symmetry in the driving force is not rigorously correct. Lacking further information, however, it is the only reasonable approximation.[28]

The best fit to this thermodynamic model is presented in Fig. 11, with the symbols corresponding to the data and the line representing a numerical solution to the equation presented in the Appendix. The rock salt phase surface energy which produced this line is given by

$$\gamma_{\mathrm{RS}}=0.63+\frac{83}{r(\text{Å})^2}\ (\text{N/m}). \tag{4}$$

The observation that the c_2 terms are approximately equal in both the rock salt and wurtzite phases ($c_{2,\mathrm{RS}}=83$, $c_{2,\mathrm{WZ}}=84$) is consistent with our assignment that this term stems from the nanocrystal curvature. The increase in the c_1, or the bulk surface energy term in the rock salt phase is, however, less intuitive. Simple calculations performed by Oshcherin[29] based only on the number of dangling bonds, the bond length, and the compressibility, predict the opposite trend. A value of $\gamma_{\mathrm{ZB}}(\mathrm{calc})=0.805$ N/m is reported for the lowest index, (111), bulk CdSe zinc blende surface, while the analogous value for the lowest index (100) bulk CdSe rock salt surface is $\gamma_{\mathrm{RS}}(\mathrm{calc})=0.69$ N/m. While experimental studies on bulk zinc blende surfaces suggest that these calculations overestimate the real value [$\gamma_{\mathrm{ZB},(111)}=0.55$ N/m (Ref. 27)], the trend with structure is probably meaningful, and our observed deviation from it needs to be explained. This topic will be addressed in the next section on kinetic effects in phase transitions.

B. Kinetics

Thermodynamics has proven to be useful in understanding the elevation in structural transformation pressure observed in CdSe nanocrystals. The anomalously high value calculated for γ_{RS} suggests that equilibrium thermodynamics are not painting a complete picture of this transformation. Kinetic, or path related effects need to be considered as well.

1. The barrier to transition in bulk CdSe

In the laboratory solid–solid transformations are usually observed to occur over a range of pressures. In addition, large differences are frequently observed between upstroke and downstroke transition pressures. These observations all point to the existence of a barrier to transition and to the fact that the temperature at which these experiments are performed is low in comparison to the height of this transition barrier. An understanding of the kinetics is thus required to correctly apply thermodynamics to this study.

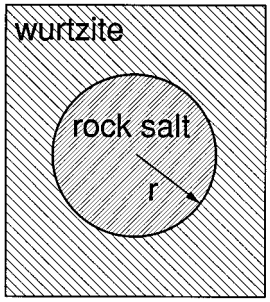

FIG. 14. Schematic representation of a rock salt nucleation domain in a bulk wurtzite lattice. The rock salt domain is destabilized by the rock salt/wurtzite interface energy. The system must be over pressurized (upstroke) or under pressurized (downstroke) to overcome this destabilization.

In high pressure studies on bulk semiconductors, the barrier to transition is usually explained in terms of nucleation dynamics.[30,31] Within this premise, the limiting step to transition is the formation of a stable nucleus of the rock salt phase within the extended wurtzite lattice (Fig. 14). This nucleus is destabilized by the rock salt/wurtzite interface energy and thus is unstable right at the thermodynamic transition pressure. At higher pressures, the rock salt nucleus is stabilized by its internal energy, and at some pressure it overcomes the interface energy and the transition occurs. On the reverse transition, the wurtzite phase nucleus is destabilized by the same rock salt/wurtzite interface energy, and so the pressure must be lowered an equivalent amount beyond the equilibrium transition pressure before the reverse transition is observed. This formalism thus predicts that the thermodynamic transition pressure will be the average of the upstroke and downstroke transition pressure. The broadening of the diffraction peaks with successive phase transitions observed in Fig. 2 for bulk CdSe is indicative of this type of mechanism where multiple nucleation sites cause a decrease in crystalline domain size upon transition.

For the case of nanocrystals however, the observation that the domain size does not significantly decrease after multiple transitions argues that this type of behavior is not occurring. From the data, we can make the conclusion that multiple stable nuclei do not coexist in the same nanocrystal. As the sizes of critical nuclei and the interactions between them are not generally known in bulk systems, these results place an important lower limit on the bulk CdSe stable nucleus size. Further experiments, related to this one, could be used to gain a more accurate idea of the forces between critical nuclei. The nanocrystal size could be increased and the experiment repeated until the domain size was no longer preserved upon transition. Work is currently underway to study phase transitions in this intermediate size range.

2. Path effects

The existence of broad hysteresis curves (Fig. 10) indicates that in our nanocrystals, and possibly in bulk systems as well, there are barriers to transition other than those associated with nucleation. In order to understand these barriers, though, we must first understand the microscopic process which leads to the transformation. In bulk systems, these atomic details are usually ignored. In a nanocrystal containing only 200 atoms, however, the motions of individual atoms must affect the dynamics of the total transformation.

While the exact nature of these motions is not well understood, Burdett has shown that much insight can be gained by using symmetry and modeling the rock salt to wurtzite transition as a Peierl's distortion.[32] In the undistorted rock salt structure, every atom is bonded to 6 other symmetry identical atoms. The system is a narrow gap semiconductor with a high electronic energy. By lengthening (i.e., breaking) two of the six bonds, and shortening the other 4, it is possible to open the band gap and decrease the electronic energy. The motion is analogous to the one-dimensional Jahn–Teller bond alternation observed in polyacetylene.[33] The rock salt to wurtzite transition in CdSe consists of this type of bond alternation in two orthogonal directions, and no distortion in the third direction. In both CdSe and polyacetylene, bond alternation opens up the band gap and reduces the overall electronic energy of the system. Under pressure, however, the total volume of the system can be reduced by reversing the Peierl's distortion. Consistent with the observation in polyacetylene,[34] the effect of pressure is to move the system toward its higher symmetry state.

This leads to the following possibility for the rock salt to wurtzite transition path: The motion can be pictured as the three-dimensional analog of the square net to graphite transition.[35] Given a repeating pattern of 2×3 rectangles, the system can distort by moving the central atoms apart to form a hexagon. In three dimensions, this distortion would be accompanied by appropriate motions in the z-direction to create cyclohexane type boats or chairs. If the final structure is zinc blende, only chair structures will form. If the final structure is wurtzite, both chairs and boats will form. The barrier to this motion is a function of the loss of octahedral bonding as the central atoms move apart, balanced against the gain in covalent sp^3 bonds as the system approaches a tetrahedral geometry. Another way to picture this motion is presented in Fig. 15 for the rock salt to wurtzite transition. Shown in part (a) are the 2×3 rectangles that will become 6 membered ring chairs in (001) planes of the wurtzite structure. The rectangles are highlighted in the rock salt cube, and the transition motions are shown for the conversion of one rectangle to a chair structure. Shown in part (b) are right angle segments of the rock salt structure that can open to form boat structures in the wurtzite phase. Finally, shown in part (c) are 2×3 rectangles that open and fold to form more wurtzite boat structures. Note that a consistent set of motions is required for all of these distortions.

Although there is no direct experimental evidence for this path, it is consistent with Burdett's theories on Peierl's distortions. Additional support is found in the observation that the acoustic shear modes in these tetrahedral semiconductors soften, that is their frequency decreases, with increasing pressure.[36] These shear modes involve atomic motions related to those described above (mostly bond angle changes[37]). The mode softening is caused by stabilization of the rock salt structure with increasing pressure. This lowers the barrier to transition and produces a broadening of the transition mode potential. It is important to note, however,

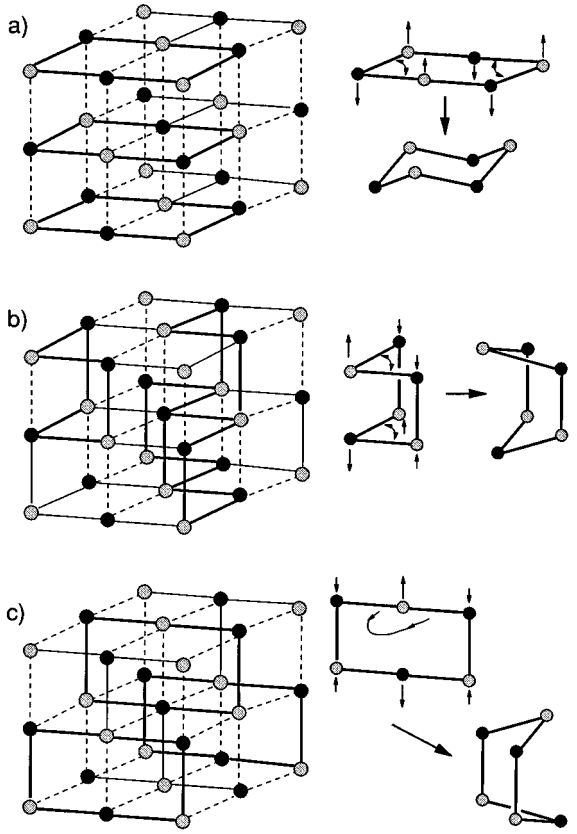

FIG. 15. Schematic representation of a possible mode for the rock salt to wurtzite transformation. (a) The middle two atoms of a 2×3 rectangle move apart and the plane puckers to produce a six membered ring ''chair'' type structure in a wurtzite (001) plane. (b) In dimensions orthogonal to (a), right angle pieces of the wurtzite structure form six membered ring ''boat'' type structure. (c) Also orthogonal to (a), 2×3 rectangles distort into wurtzite ''boat'' type structures. In all cases, 6 membered ring structures are highlighted in the rock salt lattice. These rings are then redrawn with the transition motions and final structures indicated.

that while these shear modes do soften with pressure, they do not appear to go to zero frequency at the phase transition pressure,[38] as has been observed in second order phase transitions.[39] This implies that in moving along the transition path, there is still some finite barrier to transition, even at the phase transition pressure.

3. Effect on the surface

The concept of a transition mode or path is equivalent to the statement that the connectivity of the atoms cannot completely change during a transition. As the shape of the unit cell changes upon transition, this connectivity necessitates a change in the overall shape of the crystallite. This effect is not easily observed in the bulk because the fragmentation of large crystals due to nucleation in multiple spots masks any local shape change. In nanocrystals, however, where entire crystallites transform coherently, a path driven macroscopic shape change should produce detectable results. If we assume that, as synthesized at high temperature, nanocrystals have dominantly low index surfaces, the effect of the path presented in Sec. IV B 2 above would be to convert a spherical wurtzite nanocrystal with a low surface energy into a prolate ellipsoid in the rock salt phase with a much higher surface energy.

An example of this is illustrated in Fig. 16. A two-dimensional cartoon of a wurtzite (001) plane is presented in part (a). The real (001) plane has alternate atoms displaced above and below the plane of the page. The ''surfaces'' of the plane are all low index, either the degenerate (100) or (110), and have only one dangling bond per atom. As described above, this structure can convert to a rock salt phase when atoms from across a ring come together to form a bond. This process produces a rock salt phase crystallite with (100) and (110) surfaces. In the rock salt structure, these surfaces are not degenerate. The (100) surface has only one dangling bond per atom and is thus low energy. The (110) surface, in contrast, has two dangling bonds per atom and constitutes a much higher energy surface.

Figure 16(b) shows an example of this transition path applied to a three-dimensional nanocrystal. The starting wurtzite shape is the one believed to be a typical equilibrium structure, based on TEM and Raman depolarization measurements.[14] The most striking feature of the transformation is the distinctive macroscopic shape change; the crystallite has gone from spherical to oblate. Energetically more important, however, is the fact that the newly formed rock salt crystallite has a greater number of coordinatively unsaturated surface bonds. These unsaturated bonds significantly increase the surface energy in the rock salt phase, relative to the wurtzite phase. This results in the measured elevation in phase transition pressure observed in our nanocrystals.

The change in surface energy upon transformation can be emphasized numerically by considering a very small nanocrystal, containing only 90 atoms. In the wurtzite phase of such a nanocrystal, the whole system averages 80% coordinated. That is, assuming the ideal coordination is 4, the average coordination is 3.2. This is made up of a combination of 4, 3, and 2 coordinate atoms which lie both in the interior and on the surface of the nanocrystal. When the system is moved along the proposed transition path to the rock salt structure, however, the average coordination decreases to 72%, based on an ideal coordination of 6. These changes in coordination arise because the surface structure is determined by the symmetry allowed motions of interior atoms.

Because the wurtzite structure has low symmetry in comparison to the rock salt structure, it is likely that the transformation depicted in Fig. 16(b) is unique; bond alternation (alternate bonds coming together from across a six membered ring) will always take place along the c axis and one of the degenerate a or b axes. Because of the high symmetry of the rock salt structure, however, this is not true on the reverse transition. The rock salt structure is threefold degenerate and thus bond alternation (alternate bonds breaking to form six membered rings) can occur in any two of the three directions in going from rock salt to either zinc blende or wurtzite. The inhomogeneity introduced on this reverse transition is, however, reduced by the fact that transitions to tetrahedral structures with low surface energies should be accessible at higher pressures and thus should dominate.

The anomalously high rock salt phase surface energy

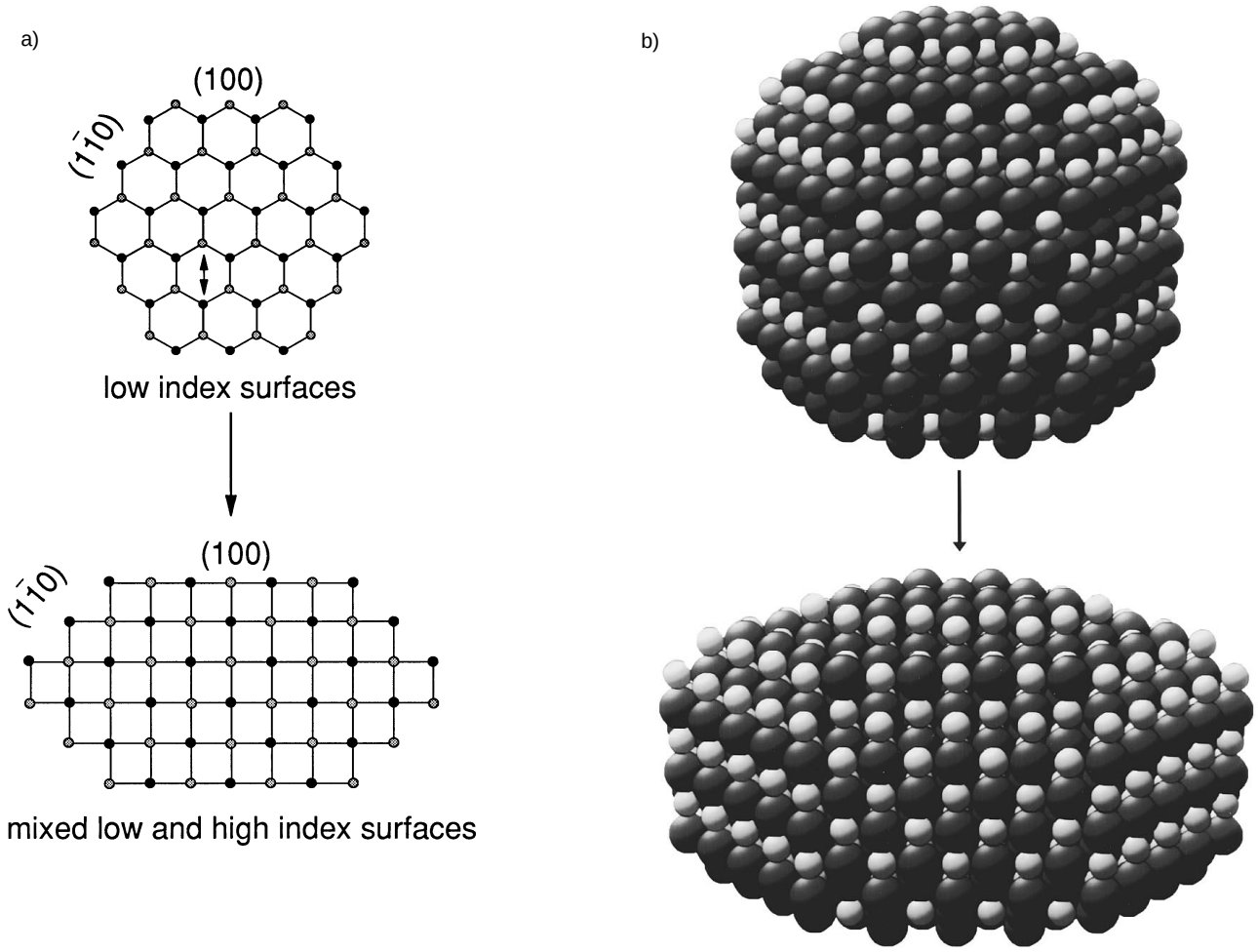

FIG. 16. (a) Transformation of a wurtzite phase nanocrystal to a rock salt phase nanocrystal following a two-dimensional analogy to the mode presented in Fig. 15(a). The wurtzite nanocrystal contains only low index ''surfaces,'' while the rock salt crystallite formed by motion along the transition path contains a large fraction of high index ''surfaces.'' (b) The same transformation, presented in 3 dimensions. The nanocrystal transforms from spherical to prolate. The transformation is accompanied by the formation of many high index surfaces in the rock salt phase. For the wurtzite phase nanocrystal, the *c* axis is vertical and in the plane of the page. The *a* and *b* axes form a 120° angle in the horizontal plane perpendicular to the page. In the rock salt phase, the *a*, *b*, and *c* axes are orthogonal and degenerate.

required to fit the size dependent phase transition data is thus a real experimental consequence of the macroscopic shape change upon transformation. While this effect can not be observed in bulk CdSe, it is probably occurring. In this way, size dependent studies of phase transitions in the nanometer regime provide information about both nanocrystal and bulk transformation kinetics. Because the surface energy in a nanocrystal makes a major contribution to the total free energy of the system, the transition path can actually determine the final state of the system. In a true equilibrium experiment, where path effects would not be important, the rock salt surface energy would probably lie below the wurtzite, and a depression of the phase transition pressure would be observed. Instead, path effects lead to higher surface energies in the rock salt phase and cause the experimentally observed elevation in phase transition pressure.

4. Hysteresis

The large hysteresis observed in Fig. 10 indicates the existence of a barrier to transition. Forward and reverse transitions do not occur at the thermodynamic transition point because extra energy must be supplied to get the system over the transition barrier. In this section we discuss the nature of this barrier and the effect of changing temperature on these transitions.

A first question is: What is the origin of this barrier? While the actual microscopic motions of interior atoms surely play a role, the hysteresis observed in CdSe nanocrystals is much greater than that observed in bulk CdSe.[7] This suggests an additional nanocrystal specific barrier to transition. A useful body of literature to help in answering this question concerns martensitic transformations. These are temperature or pressure induced solid–solid phase transitions that can be described in terms of a soft mode picture, and which are marked by hysteresis.[40] One key feature of these transitions is that the extent of transformation can be described in terms of state variables.[41] That is, at a given T and P beyond the equilibrium transition point, the extent of transformation will be a function of T and P, and not of the time spent at those conditions. This allows the application of

quasiequilibrium thermodynamics to describe the under- or overpressurized system. In this formalism, the width of the hysteresis curve (i.e., the difference between $P_{\text{trans,up}}$ and $P_{\text{trans,down}}$) is assigned to nonreversible, non-PV work. Microscopically, this hysteresis in Martensitic transformations can be related to inelastic atomic rearrangements.[41] The motions of interior atoms in our nanocrystals should be dominantly elastic and the energy stored in the rock salt lattice should be recoverable upon release of pressure. This leaves the nonreversible, inelastic rearrangement of surface atoms to explain the extra width of the nanocrystal hysteresis. The rearrangements could include surface reconstruction, or the breaking of surface Cd–pyridine, CdO_x, or SeO_x bonds to accommodate the new interior structure.

For clarity, it should be emphasized that there are two separate concepts in surface energy being presented here. The notion of a path driven increase in surface energy (Sec. IV B 3) is a thermodynamic idea, and corresponds to a reversible storage of energy in the lattice. This value is thus calculated from the midpoint of the hysteresis curves. The notion of nonreversible surface atom rearrangements is a nonequilibrium idea, and relates only to the width of the hysteresis curves, not the center point.

One experimental difficulty with this picture is that the recovered tetrahedral phase surface energy is not required to be exactly the same as the original wurtzite surface energy. If this recovered surface energy were higher than the original wurtzite phase surface energy (a physically reasonable assumption), some of the driving force for the reverse transition would be removed. In this case, the apparent width of the hysteresis curves would be an overestimate of the real situation. The additional width could be caused by the fact that the upstroke ''thermodynamic'' transition point differed from the downstroke ''thermodynamic'' transition point. While this idea is not unreasonable or inconsistent with the data, there is no practical way to incorporate it into the analysis of the data. Absent surface-structure specific high pressure data, we will continue to use the simplifying assumption that the surface energy in the recovered phase is the same as in the untransformed nanocrystals.

Another point of interest is to consider the effect of temperature on the hysteresis. At room temperature, the barrier to transition appears be large in comparison to kT. It should be possible, however, to raise the temperature to the point that the barrier height is on the order of kT. In this situation, if the temperature is low enough that diffusion of surface atoms is still slow, little hysteresis would be expected and the observed upstroke transition pressures should correlate well with our measured thermodynamic transition pressure. If, however, the temperature is high enough that the diffusion of surface atoms becomes fast on the time scale of the phase transition, high pressure phase nanocrystals with a true equilibrium, low energy surface could be formed. In this case, the phase transition pressure should decrease to the point determined by the difference in the equilibrium rock salt and wurtzite surface energies. This reasoning suggests that the experiments presented here should not, in fact, even be called quasiequilibrium; not only are the nanocrystallites themselves kinetically trapped high energy structures, but the phase transition pressures we have determined are path, and thus temperature dependent quantities.

This result has implications not only for nanocrystals, but also for phase transitions in bulk materials at room temperature. In the first place, the path driven surface and shape effects described above should play an important role in bulk nucleation. As previously discussed, the hysteresis in bulk transitions is believed to stem from an interface energy associated with a nucleus of phase I in bulk phase II (Fig. 14). This interface energy should be strongly affected by the surface structure of the transformed phase I nucleus, and by the shape mismatch between the phase I nucleus and the phase II cavity. These effects are traditionally ignored in nucleation theories of phase transitions.[30,31] A knowledge of these surface and shape effects is required for a full understanding of the role of nucleation in hysteresis. Perhaps more important, however, is the concept that path driven changes in surface energy can effect measured phase transition pressures. In bulk systems which have undergone more than one solid–solid phase transition, the domains can reach the size where surface energies make a significant contribution to the total free energy of the system. As a consequence, samples that have been repeatedly pressure cycled do not give reproducible hysteresis loops. Therefore, experimentally determined phase transition pressures at room temperature are not necessarily a good measure of the relative stability of various bulk phases.

The path dependence and hysteresis of the phase transition pressure could, however, be exploited for potential applications. In the high temperature high pressure experiment described previously, the temperature could be slowly reduced while the nanocrystals were still in the high pressure rock salt phase. The result would be the formation of a low energy equilibrium surface in the rock salt phase. In contrast to the present experiment, the effect of this surface would be to stabilize the high pressure phase with respect to the low pressure phase upon release of pressure. Under the right conditions, it should even be possible to trap CdSe nanocrystals in the rock salt structure at atmospheric pressure and room temperature. Alternatively, surface capping groups and pressure media could be chosen to stabilize the rock salt phase nanocrystals. If wurtzite phase nanocrystals could be dissolved in such a medium, the possibility again exists for recovery of rock salt phase nanocrystals at atmospheric pressure and room temperature after pressurization. This idea is supported by recent results by Lin *et al.*[42] who have stabilized cube shaped rock salt phase CdS nanocrystals of 100 nm diam by growing them in a highly ionic polymer matrix. In this way, surface energies and transition barriers can be used to tune the stable states of matter in the nanometer size regime.

V. CONCLUSIONS

In this paper we have examined the effect of finite size on the high pressure stability of CdSe semiconductor nanocrystals. While the nanocrystals do undergo a wurtzite to rock salt transition that is analogous to that observed in bulk CdSe, it is found that the limited extent of the crystallites affects both the thermodynamics and kinetics of the transi-

tion. The basic nature of the transition, determined using high pressure X-ray powder diffraction, shows a clean transition from a wurtzite phase to a rock salt phase, and back to a mixed wurtzite/zinc blende phase with no significant loss of crystalline domain size. The transition in the nanocrystals, however, takes place at pressures much higher than those observed for bulk CdSe.

A thermodynamic analysis of the phase transition pressure allows for the determination of the surface energy in the high pressure phase. This value is found to be $\gamma_{RS}=0.63+83/r(\text{Å})^2$ (N/m), in comparison with a value of $\gamma_{WZ}=0.34+84/r(\text{Å})^2$ (N/m) obtained using the Laplace Law for the low pressure phase. This large rock salt surface energy can be attributed in part to high index surfaces formed at the transition because of the dynamic path atoms must travel to move from one structure to the other. This result suggests that nanocrystal surfaces formed during solid–solid phase transitions are nonequilibrium, and thus phase transformations of this sort are not well suited for the determination of stable *equilibrium* structures in finite size. As bulk systems approach this size regime, where surface energy terms become an important part of the total free energy, these effects need to be considered.

The transition kinetics are also affected by finite size. Broad hysteresis curves suggest significant barriers to transition in nanocrystals. It appears, however, that nanocrystals may be smaller than the critical nuclei hypothesized to provide the barrier to transition in bulk semiconductors. Nucleation, therefore, does not control to the transition barrier in these systems. This result can be used to gain understanding of the effect of nucleation in bulk CdSe.

The nanocrystal surface is shown to be important to both the thermodynamics and kinetics of the transformation. The surface energy, whether thermodynamic or the result of a kinetic process, appears to be the dominant factor in determining stable states in finite sized systems. Despite this fact, the basic nature of the transition remains bulklike. The differences between transformations in finite systems and those in the bulk can be used to understand the evolution of solid–solid phase transitions from the bulk limit into a coherent molecular isomerization. This information can add both to our basic understanding of phase transitions in solids, and to our comprehension of the role of physical size in the stability of a crystallite.

ACKNOWLEDGMENTS

The authors wish to thank Dr. Malcolm Nicol and Suzanna Gibson for their technical assistance with this experiment. A.P.A. acknowledges an Alfred P. Sloan Foundation Fellowship. This work has been partially supported by the donors of the Petroleum Research Fund, administered by the American Chemical Society, and by the Director, Office of Energy Research, Office of Basic Energy Sciences, Materials Sciences Division, of the U.S. Department of Energy under Contract No. DE-AC03-76SF00098. These experiments were performed using the facilities of the University of California-Lawrence Livermore National Lab PRT at the Stanford Synchrotron Radiation Laboratory, which is operated by the Department of Energy, Division of Chemical Sciences.

APPENDIX

For the bulk system, the internal energy in the high and low pressure phases is given by

$$\begin{aligned} U_{WZ}(T,P) &= TS_{WZ}(T,P) - PV_{WZ} + \mu_{WZ}N_{WZ}, \\ U_{RS}(T,P) &= TS_{RS}(T,P) - PV_{RS} + \mu_{RS}N_{RS}, \end{aligned} \tag{A1}$$

where U, S, and μ are the internal energy, entropy, and chemical potential, respectively, for each phase. In the case of nanocrystals, Eq. (A1) must be modified by a surface energy term,

$$\begin{aligned} U_{WZ}(P,V) &= TS_{WZ} - PV_{WZ} + \mu_{WZ}N_{WZ} - \gamma_{WZ}A_{WZ}, \\ U_{RS}(P,V) &= TS_{RS} - PV_{RS} + \mu_{RS}N_{RS} - \gamma_{RS}A_{RS}, \end{aligned} \tag{A2}$$

where γ_i and A_i are the surface tension and surface area, respectively, in phase i. Experimentally,[43] it has been observed that the entropy change upon transition is small, so the TS_i terms in Eqs. (A1) and (A2) are frequently dropped in actual calculations of thermodynamic parameters. Given that the condition for a phase transition to occur is $\mu_{wz}=\mu_{RS}$, the necessary condition for a phase transition in a nanocrystal system is given by

$$P_T(V_{WZ}-V_{RS}) + U_{WZ}(P_T) - U_{RS}(P_T) = \gamma_{RS}A_{RS} - \gamma_{WZ}A_{RS}, \tag{A3}$$

where P_T is the nanocrystal phase transition pressure. Equation (A3) can be used in combination with a knowledge of the volume compressibility in both phases to generate the energy volume curves (Fig. 12). This allows for experimental determination of the surface energy (γ).

The first term in Eq. (A3) can be calculated using the Murnaghan equations of state[44] in combination with measured CdSe nanocrystal compressibility constants. For the wurtzite phase, compressibility constants were obtained from high pressure EXAFS experiments carried out on 2.7 nm radius CdSe nanocrystals.[13] The resultant values for the bulk modulus and its derivative with respect to pressure are $B_0=37\pm5$ GPa and $B_0' = 11 \pm 3$. The compressibility constant for the rock salt phase is obtained from this work, $B_0=74\pm2$ GPa. As the data are observed to vary quite linearly with pressure, the rock salt data was not fit with a B_0' value. Note that the size dependence in Eq. (A3) arises both from the variation of P_T with nanocrystal size, and from the nanocrystal surface energy, which is size dependent and gives rise to an effective pressure which in turn modifies the applied pressure. The relevant volume equations needed to calculate the first term in Eq. (A3) for each phase are

$$V_{WZ}(P_T, r_{WZ}) = \frac{V_{0,WZ}}{\left[1 + \frac{B_0'}{B_{0,WZ}} \cdot \left(P + \frac{2\gamma_{WZ}}{r_{WZ}}\right)\right]^{1/B_0'}}, \tag{A4}$$

$$V_{\mathrm{RS}}(P_T, r_{\mathrm{RS}}) = \frac{V_{0,\mathrm{RS}}}{\left[1 + \frac{1}{B_{0,\mathrm{RS}}} \cdot \left(P + \frac{2\gamma_{\mathrm{RS}}}{r_{\mathrm{RS}}}\right)\right]}, \tag{A5}$$

where the V_0 term for Eq. (A4) is obtained from bulk CdSe at atmospheric pressure. In Eq. (A5), the V_0 term is obtained by extrapolation of bond length vs pressure data from this paper for a large size nanocrystal sample to atmospheric pressure. While this value will deviate slightly from the bulk value because of the surface pressure on the clusters, the large size of the sample makes the error introduced by this approximation small. The nanocrystal radius in the high pressure phase (r_{RS}) is calculated from the volume contraction assuming spherical nanocrystals. This, however, leads to a recursive formula for the high pressure phase volume. Thus, after one level of recursion, r_{RS} is fixed at $0.75^{1/3}$ times the wurtzite phase radius, which is the value observed experimentally for 2.7 nm crystallites from high pressure EXAFS.[15]

The second term in Eq. (A3) must be broken into two parts to obtain numerical values,

$$\begin{aligned} U_{\mathrm{WZ}}(P_T) - U_{\mathrm{RS}}(P_T) = &[U_{\mathrm{WZ}}(P_T) - U_{\mathrm{WZ}}(P_B)] \\ &- [U_{\mathrm{RS}}(P_T) - U_{\mathrm{RS}}(P_B)] \\ &+ U_{\mathrm{WZ}}(P_B) - U_{\mathrm{RS}}(P_B), \end{aligned} \tag{A6}$$

where P_B is the bulk phase transition pressure. By setting the chemical potentials equal in Eq. (A1), it is shown that

$$U_{\mathrm{WZ}}(P_B) - U_{\mathrm{RS}}(P_B) = -P_B[V_{\mathrm{WZ}}(P_B) - V_{\mathrm{RS}}(P_B)] \tag{A7}$$

and thus the last two terms in Eq. (A6) can be calculated from the bulk CdSe phase transition pressure and the volume change at transition in the bulk system. The middle two terms in Eq. (A6) (square brackets) can be calculated by integrating the Murnaghan equations of state [Eqs. (A4) and (A5)] to generate energy–volume curves. The explicit forms of these curves for the wurtzite and rock salt phases (i.e., with and without B_0') can be obtained and are presented in Eqs. (A8) and (A9),

$$\begin{aligned} E_{\mathrm{WZ}}(V) &= -\int_{P_B}^{P_T} P dV_{\mathrm{WZ}} \\ &= \frac{B_{0,\mathrm{WZ}}}{B_0'} V_{\mathrm{WZ}} \cdot \left\{1 + \left[\frac{(V_{0,\mathrm{WZ}}/V_{\mathrm{WZ}})^{B_0'}}{(B_0' - 1)}\right]\right\}\Bigg|_{P_B}^{P_T}, \end{aligned} \tag{A8}$$

$$\begin{aligned} E_{\mathrm{RS}}(V) &= -\int_{P_B}^{P_T} P dV_{\mathrm{RS}} \\ &= (B_{0,\mathrm{RS}} \cdot V_{\mathrm{RS}}) - [B_{0,\mathrm{RS}} \cdot V_{0,\mathrm{RS}} \cdot \ln(V_{\mathrm{RS}})]\Big|_{P_B}^{P_T}. \end{aligned} \tag{A9}$$

The nanocrystal size dependence in these equations stems both from the direct dependence on P_T and from the size dependence of the volume.

The final term in Eq. (A3) depends only upon the nanocrystal surface area and the surface tension. The surface area in each phase is calculated from the volume assuming spherical crystallites. The best form for the surface tension (γ) is discussed at some length in Sec. IV A 1 of the discussion and thus will not be repeated here.

This combination of approximations and substitutions, in combination with the constants in Table I, allows for numerical evaluation of all of the terms in Eq. (A3) except the rock salt phase surface energy. This is used in Sec. IV A 2 to compare this thermodynamic model to the size dependent phase transition data collected on a variety of nanocrystals.

[1] This type of behavior has been observed in a variety of very different clusters. Examples of novel bonding geometries in covalent, metallic, and ionic clusters include H. W. Kroto, J. R. Heath, S. C. O'Brien, R. F. Curl, and R. E. Smalley, Nature **318**, 162 (1985); B. K. Teo, X. Shi, and H. Zhang, J. Am. Chem. Soc. **113**, 4329 (1991); J. Deifenbach and T. P. Martin, J. Chem. Phys. **83**, 4585 (1985).

[2] A. N. Goldstein, C. M. Echer, and A. P. Alivisatos, Science **256**, 1425 (1992).

[3] C. J. Coombes, J. Phys. **2**, 441 (1972); P. Buffat and J.-P. Borel, Phys. Rev. A **13**, 2287 (1976).

[4] S. H. Tolbert and A. P. Alivisatos, Science **265**, 373 (1994).

[5] C. B. Murray, D. J. Norris, and M. G. Bawendi, J. Am. Chem. Soc. **115**, 8706 (1993).

[6] J. E. Bowen Katari, V. L. Colvin, and A. P. Alivisatos, J. Phys. Chem. **98**, 4109 (1994).

[7] For the these experiments we have defined the thermodynamic phase transition pressure as the midpoint of the hysteresis curve, or equivalently the average of the upstroke and downstroke transition pressures. This produces a bulk CdSe transition pressure of 2 GPa, in comparison to the upstroke value of 3 GPa. Experiments on bulk CdSe which show full hysteresis data include (a) A. L. Edwards and H. G. Drickamer, Phys. Rev. **122**, 1149 (1961); (b) A. Onodera, Rev. Phys. Chem. Jpn. **39**, 65 (1969); (c) W. C. Yu and P. J. Gielisse, Mater. Res. Bull. **6**, 621 (1971).

[8] A. P. Alivisatos, T. D. Harris, L. E. Brus, and A. Jayaraman, J. Chem. Phys. **89**, 5979 (1988).

[9] S. H. Tolbert and A. P. Alivisatos, Z. Phys. D **26**, 56 (1993).

[10] M. Haase and A. P. Alivisatos, J. Phys. Chem. **96**, 6756 (1992).

[11] X. S. Zhao, J. Schroeder, P. D. Persans, and T. G. Bilodeau, Phys. Rev. B **43**, 12 580 (1991).

[12] L. J. Cui, U. D. Venkateswaran, B. A. Weinstein, and F. A. Chambers, Phys. Rev. B **45**, 9248 (1992).

[13] S. H. Tolbert and A. P. Alivisatos, in *NATO ASI Proceedings on Nanophase Materials: Synthesis-Properties-Applications*, edited by G. C. Hadjipanayis and R. W. Siegel (Kluwer Academic, Dordrecht, 1993), pp. 471–482.

[14] J. J. Shiang, A. V. Kadavanich, R. K. Grubbs, and A. P. Alivisatos (unpublished).

[15] L. R. Becerra, C. B. Murray, R. G. Griffin, and M. G. Bawendi, J. Chem. Phys. **100**, 3297 (1994).

[16] JCPDS-ICDD powder pattern card #8-459, (c) 1989.

[17] JCPDS-ICDD powder pattern card #21-829, (c) 1989; J. Osugi, K. Shimizu, T. Nakamura, and A. Onodera, Rev. Phys. Chem. Jpn. **36**, 59 (1966).

[18] A. N. Mariano and E. P. Warekois, Science **142**, 672 (1963).

[19] JCPDS-ICDD powder pattern card #19-191, (c) 1989.

[20] R. A. Montalvo and D. W. Langer, J. Appl. Phys. **41**, 4101 (1970); C. F. Cline and D. R. Stephens, *ibid*. **36**, 2869 (1965).

[21] S. H. Tolbert, A. B. Herhold, C. S. Johnson, and A. P. Alivisatos, Phys. Rev. Lett. **73**, 3266 (1994).

[22] J. A. Corll, J. Appl. Phys. **35**, 3032 (1964).

[23] I. Szleifer, D. Kramer, A. Ben-Shaul, W. M. Gelbart, and S. A. Safran, J. Chem. Phys. **92**, 6800 (1990).

[24] For a review of these ideas see R. S. Berry, S. A. Rice, and J. Ross, *Physical Chemistry* (Wiley, New York, 1980), pp. 875–883.

[25] C. Solliard and M. Flueli, Surf. Sci. **156**, 487 (1985).

[26] F. Grieser, G. Mills, and D. Meisel, J. Colloid Interface Sci. **120**, 540 (1987).

[27] B. F. Ordmont, Dokl. Akad. Nauk. SSSR **124**, 132 (1959); S. N. Sadumkin, Fiz. Tverd. Tela **2**, 880 (1960).

[28] X. Li and R. Jeanloz, Phys. Rev. B **36**, 474 (1987); R. Jeanloz, J. Geophys. Res. **79**, 10 352 (1987).

[29] B. N. Oshcherin, Phys. Status Solidi A **34**, K181 (1976).

[30] R. E. Hanneman, M. D. Banus, and H. C. Gatos, J. Phys. Chem. Solids **25**, 293 (1964).
[31] U. D. Venkateswaran, L. J. Cui, B. A. Weinstein, and F. A. Chambers, Phys. Rev. B **45**, 9237 (1992).
[32] J. K. Burdett and T. J. McLarnan, J. Chem. Phys. **75**, 5765 (1981); J. K. Burdett, Prog. Solid State Chem. **15**, 173 (1984).
[33] J. Ma, J. E. Fischer, Y. Cao, and A. J. Heeger, Solid State Commun. **83**, 395 (1992).
[34] D. Moses, A. Feldblum, E. Ehrenfreund, A. J. Heeger, T.-C. Chung, and A. G. MacDiarmid, Phys. Rev. B **26**, 3361 (1982); A. Brillante, M. Hanfland, K. Syassen, and J. Hocker, Physica B & C **139 & 140**, 533 (1986).
[35] J. K. Burdett, and S. Lee, J. Am. Chem. Soc. **105**, 1079 (1983).
[36] B. A Weinstein, in *High Pressure Science and Technology*, edited by K. D. Timmerhaus and M. S. Barber (Plenum, New York, 1979), Vol. 1, p. 141.
[37] D. J. Chadi and R. M. Martin, Solid State Commun. **19**, 643 (1976).
[38] S.-K. Chan, Mater. Sci. Forum **56–58**, 101 (1990).
[39] T. P. Dougherty, G. P. Wiederrecht, K. A. Nelson, M. H. Garrett, H. P. Jensen, and C. Warde, Science **258**, 770 (1992).
[40] N. Nakanishi, A. Nagasawa, and Y. Murakami, J. Phys. (Paris) **43**, C4-35 (1982).
[41] P. Wollants, J. R. Roos, and L. Delaey, Prog. Mater. Sci. **37**, 227 (1993).
[42] J. Lin, E. Cates, and P. A. Bianconi, J. Am. Chem. Soc. **116**, 4738 (1994).
[43] M. Bockowski, S. Krukowski, and B. Lucznik, Semicond. Sci. Technol. **7**, 994 (1992).
[44] F. D. Murnaghan, Proc. Natl. Acad. Sci. USA **30**, 224 (1944).